Brain Struct Funct (2016) 221:2589–2605
DOI 10.1007/s00429-015-1060-5

ORIGINAL ARTICLE

Multimodal connectivity mapping of the human left anterior and posterior lateral prefrontal cortex

Andrew T. Reid[1] · Danilo Bzdok[1,2,7] · Robert Langner[1,2] · Peter T. Fox[4,8] · Angela R. Laird[5] · Katrin Amunts[1,6] · Simon B. Eickhoff[1,2] · Claudia R. Eickhoff[1,3]

Received: 7 October 2014 / Accepted: 7 May 2015 / Published online: 16 May 2015

Abstract Working memory is essential for many of our distinctly human abilities, including reasoning, problem solving, and planning. Research spanning many decades has helped to refine our understanding of this high-level function as comprising several hierarchically organized components, some which maintain information in the conscious mind, and others which manipulate and reorganize this information in useful ways. In the neocortex, these processes are likely implemented by a distributed frontoparietal network, with more posterior regions serving to maintain volatile information, and more anterior regions subserving the manipulation of this information. Recent meta-analytic findings have identified the anterior lateral prefrontal cortex, in particular, as being generally engaged by working memory tasks, while the posterior lateral prefrontal cortex was more strongly associated with the cognitive load required by these tasks. These findings suggest specific roles for these regions in the cognitive control processes underlying working memory. To further characterize these regions, we applied three distinct seed-based methods for determining cortical connectivity. Specifically, we employed meta-analytic connectivity mapping across task-based fMRI experiments, resting-state BOLD correlations, and VBM-based structural covariance. We found a frontoparietal pattern of convergence which strongly resembled the working memory networks identified in previous research. A contrast between anterior and posterior parts of the lateral prefrontal cortex revealed distinct connectivity patterns consistent with the idea of a hierarchical organization of frontoparietal networks. Moreover, we found a distributed network that was anticorrelated with the anterior seed region, which included most of the default mode network and a subcomponent related to social and emotional processing. These findings fit well with the internal attention model of working memory, in which representation of information is processed according to an anteroposterior gradient of abstract-to-concrete representations.

Keywords Meta-analytic connectivity modeling · Functional connectivity · Structural covariance · Working memory · Anterior lateral prefrontal cortex · Posterior lateral prefrontal cortex

Electronic supplementary material The online version of this article (doi:10.1007/s00429-015-1060-5) contains supplementary material, which is available to authorized users.

✉ Andrew T. Reid
a.reid@fz-juelich.de

[1] Institute of Neuroscience and Medicine (INM-1), Research Centre Jülich, Jülich, Germany

[2] Institute of Clinical Neuroscience and Medical Psychology, Heinrich Heine University, Düsseldorf, Germany

[3] Department of Psychiatry, Psychotherapy and Psychosomatics, University Hospital Aachen, Aachen, Germany

[4] University of Texas Health Sciences Center at San Antonio, San Antonio, TX, USA

[5] Florida International University, Miami, FL, USA

[6] C. & O. Vogt Institute for Brain Research, Heinrich Heine University, Düsseldorf, Germany

[7] Parietal Team, INRIA, Neurospin, Bat 145, CEA Saclay, 91191 Gif-Sur-Yvette, France

[8] South Texas Veterans Health Care System, San Antonio, TX, USA

Introduction

Working memory (WM) is a high-level cognitive function that maintains and manipulates transient representations of relevant information, and is critical for reasoning, problem

solving, and executive control of action. WM can be broadly divided into two subcomponents (Fletcher and Henson 2001): maintenance, in which volatile information is kept in mind without external reinforcement; and manipulation, in which bits of information are reorganized or otherwise modified. Perhaps the most influential model of WM was first proposed by Baddeley and Hitch (1974), and comprised several components: the phonological loop, which subserves processing of short-term linguistic information; the visuospatial sketchpad, which performs similar operations on visual and spatial information; the central executive, an attentional process which controls the flow of information to and from these components; and the episodic buffer, which retains the temporal sequence of currently experienced events, and establishes links to long-term episodic memory (Baddeley 2000, 2003; Baddeley and Hitch 1974). The anatomical bases for this WM model were originally elucidated through lesion studies (reviewed in Stuss 2006), and have been more recently refined through neuroimaging evidence (Fletcher and Henson 2001; Lückmann et al. 2014). These findings suggest that WM is subserved by distinct, interacting modules, which are located primarily in the lateral prefrontal (LPFC) and superior parietal cortices.

With the aim of refining the localization of WM-related processes, we previously performed a coordinate-based meta-analysis using activation likelihood estimation (ALE; Eickhoff et al. 2009) across functional magnetic resonance imaging (fMRI) studies on WM (Rottschy et al. 2012). This approach offers two main advantages over individual task-based studies. Firstly, since individual tasks can only ever partially capture the neural substrates of the psychological process under investigation, meta-analysis provides a means of establishing convergence across many laboratories and experimental paradigms. Secondly, meta-analysis can compile information from a large number of experiments and subjects, which allows it more statistical power than single studies can typically obtain. Our meta-analysis highlighted a network of regions including the lateral prefrontal (LPFC) and frontal cortex, the premotor cortex (PMC), the anterior insula, the middle cingulate cortex (MCC), the superior parietal lobule (SPL), and the intraparietal sulcus (IPS). This study also revealed a clear distinction in the neural correlates of WM for studies testing WM per se (against a baseline or control condition; *task-set* effects) and studies which assessed the neural correlates of increasing WM load or difficulty (e.g., 3-back versus 1-back tasks; *task-load* effects). Comparing activations reported for task-set effects to those for task-load effects revealed stronger convergence among the former in the left anterior LPFC (aLPFC), bilateral anterior insula, and right SPL/IPS, while the latter showed stronger convergence in the bilateral posterior LPFC (pLPFC) and MCC.

This distinction of WM-related activation into task-set and task-load components supports the idea of a modular organization, with task-load components having a maintenance role and task-set components subserving the manipulation of information flow. It has been suggested that WM is dependent on internal attention processes driven by top-down modulation (Awh and Jonides 2001; Gazzaley and Nobre 2012). Internal attention is likely mediated by the so-called "dorsal attention network" (DAN), which overlaps with the task-set network identified in our previous analysis—particularly, in PMC and IPS/SPL (Barrett et al. 2004; Lückmann et al. 2014). The DAN has been proposed by Lückmann and colleagues to subserve an overarching control mechanism consistent with activation patterns in WM, long-term memory consolidation, and visual imagery—possibly through the top-down control of sustained oscillatory activity in lower-level circuits. The importance of these regions for the attentional manipulation of information, rather than its maintenance, is substantiated through fMRI (Corbetta et al. 2002), lesion studies (Berryhill et al. 2011; du Boisgueheneuc et al. 2006) and repetitive transcranial magnetic stimulation (rTMS) applied simultaneously with fMRI acquisition (Hamidi et al. 2008; Postle et al. 2006). Specifically, lesions to posterior parietal regions, but not dorsolateral PFC, reduce WM capacity, but dorsolateral PFC lesions do impair performance on delayed-response WM tasks, which are thought to rely more on verbal rehearsal (D'Esposito and Postle 1999). Interestingly, in the Rottschy et al. (2012) study, task-set regions generally overlapped with task-load regions, indicating an association between task complexity and the level of activation. In contrast, this overlap did not include the left aLPFC. This region was highlighted by Koechlin et al. (1999) as being activated only when a subject was required to maintain a goal in mind while executing several subgoals (so-called branching tasks). Neither maintaining a single goal nor performing subsequent independent subgoals was sufficient to activate this region. Also using fMRI, Rowe et al. (2000) reported that the aLPFC was associated specifically with the selection of information from WM, rather than its maintenance. These observations suggest that the aLPFC operates as a higher-level coordinator of the attentional mechanisms described above.

In addition to these positive relationships between WM and neural activity, fMRI activity in certain cortical regions has been robustly shown to decrease in the presence of WM task demands, and increase in their absence. This so-called "default mode network" (DMN) comprises primarily medial prefrontal and parietal regions (posterior cingulate, retrosplenial cortex, temporoparietal junction, and medial PFC) (Buckner et al. 2008; Raichle et al. 2001). The DMN has been consistently shown to be anticorrelated

with the DAN, and this antagonistic relationship may represent competing neural demands on the focused attention required for demanding tasks such as are commonly employed to assess WM, and the more free-flowing inventory appraisal and cognitive remodeling which may be occurring in the DMN-associated brain state (Fox et al. 2005; Mason et al. 2007; Sridharan et al. 2008; Weissman et al. 2006). Several functions have been proposed for the DMN, including mind-wandering (Mason et al. 2007), autobiographical memory, spatial navigation, and theory of mind (Spreng and Grady 2009), and general social cognition (Mars et al. 2012; Schilbach et al. 2008). In a recent ALE meta-analysis, regions with reduced activations relative to resting-state conditions (DMN) overlapped with those associated with social and emotional processing (EMO), specifically in the precuneus and dorsomedial PFC (Schilbach et al. 2012). This and other evidence has led to the suggestion that DMN has a role in processing social and emotional information and that this process is antagonistic with tasks requiring focused internal attention, such as WM (Lückmann et al. 2014).

Both aLPFC and pLPFC are likely to have broader roles in cognitive control, of which WM is an important component. Several lines of evidence, including lesion studies (Badre et al., 2009) and task-based fMRI (Koechlin et al. 2003) have led to the proposal that LPFC is organized along its anteroposterior axis from representing more abstract, temporally broad information (anterior), to more concrete, immediate information (posterior). Furthermore, this organization is likely hierarchical, with higher-level anterior regions biasing or manipulating the information provided by lower-level posterior regions, but not vice versa (Badre 2008; Christoff and Gabrieli 2013; Koechlin and Summerfield 2007). In other words, the LPFC and regions communicating with it may be arranged as a set of nested, interacting components, with concrete information being transformed into increasingly abstract representations at each subsequent component, and high-level contextual and goal-driven information being used to manipulate the flow of this bottom-up stream. Consistent with this model, Lee et al. (2013) showed that, while BOLD activations during a visual task encode the visual stimulus in striate cortex, activations while processing more abstract information (categorization of words) encode this information in the LPFC. Within the LPFC itself, activity in aLPFC was found to more likely represent internally generated information, as shown by event-related fMRI evidence, while pLPFC activity represented more externally generated information (Christoff et al. 2003).

The foregoing evidence supports the hypothesis that the left aLPFC has a distinct role in the coordination of attentional and cognitive control processes in WM, and predicts that it will have strong associations with regions of the task-set and task-load networks, despite having no apparent load dependence itself. Furthermore, the reported antagonism between WM- and DMN-related processes predicts negative associations between aLPFC and DMN or EMO regions. Posterior LPFC likely plays an intermediary role in this process; being at a lower hierarchical level than its anterior counterpart predicts that its connectivity profile will involve lower-level regions processing more concrete representations of sensory or motor information. In the present study, we investigated these relationships by computing functional networks that were either positively or negatively associated with the left aLPFC and pLPFC. Several proxy measures have been proposed which attempt to relate associations in MRI signals to the underlying functional communication between brain regions, mediated by axonal connections. However, each of these methods captures unique spatial and temporal patterns of association, since they represent conceptually different phenomena, and are subject to different types of preprocessing requirements and measurement noise. Comparing the evidence across these modalities allows us to quantify their shared variance, and yields a robust "core" functional connectivity network. Accordingly, we compare proxy measures of connectivity based upon three distinct imaging methodologies: meta-analytic connectivity modeling (MACM), resting-state fMRI connectivity (RS-FC), and structural covariance (SC).

Materials and methods

Seed identification and anatomical labeling

The putative role of the left aLPFC in coordinating and selecting WM processes indicates that it should have connectivity with both task-set and task-load components of the WM network. Additionally, the putative intermediary role of pLPFC predicts it will be more associated with lower-level regions outside the core WM network. To investigate these predictions, the left aLPFC and pLPFC (Fig. 1) were taken as seed regions for further analysis of task-dependent (MACM) and task-independent (resting state) functional connectivity, as well as structural covariance (SC) analysis (Eickhoff et al. 2010). In both cases, the seed regions were derived from the thresholded (at cluster-level family-wise-error-corrected $p < 0.05$) statistical maps from Rottschy et al. (2012), with the aLPFC cluster's peak being located at MNI coordinates [−38, 50, 12], and pLPFC's at [−48, 24, 30]. These peak coordinates are reported as a convenient reference, while the entire suprathreshold clusters were used as seed regions. All results were anatomically labeled by reference to probabilistic cytoarchitectonic maps of the human brain

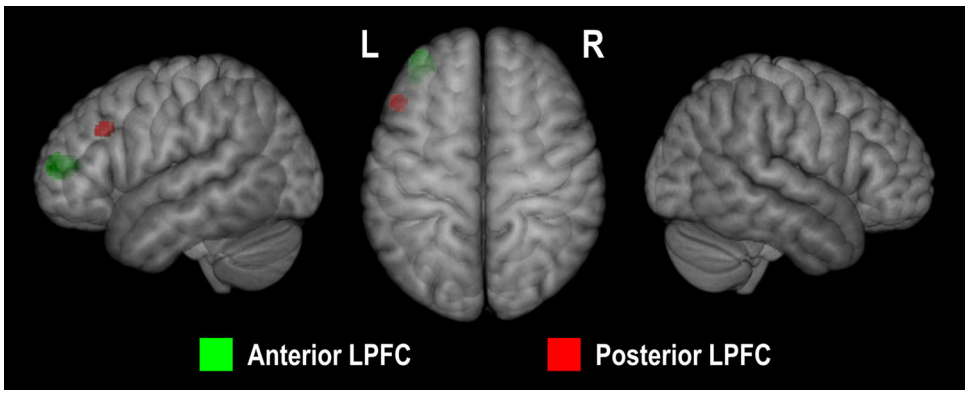

Fig. 1 The left aLPFC and pLPFC seed regions used for MACM, RS-fMRI, and SC connectivity analyses

using the SPM Anatomy Toolbox (Eickhoff et al. 2005, 2006, 2007). Using a Maximum Probability Map (MPM), activations were assigned to the most probable histological area at their respective locations. Details on these cytoarchitectonic regions are found in the following publications reporting on Broca's region (Amunts et al. 1999), inferior parietal cortex (Caspers et al. 2006, 2008), superior parietal cortex, and intraparietal sulcus (Choi et al. 2006; Scheperjans et al. 2008a, b). Regions which are not yet cytoarchitectonically mapped based on observer-independent histological examination were labeled macroanatomically by the probabilistic Harvard-Oxford cortical structural atlas (Desikan et al. 2006), rather than providing tentative histological labels based on volume-approximations of the (schematic) Brodmann atlas. Note that the terms "anterior" and "posterior" are used hereafter, instead of the (equivalent terms) "rostral" and "caudal", as used in Rottschy et al. (2012).

Meta-analytic connectivity modeling (MACM)

Functional connectivity of the seed during task performance was delineated by meta-analytic connectivity modeling (MACM). This approach to functional connectivity assesses which brain regions are co-activated above chance with a particular seed region in functional neuroimaging experiments. The first step in MACM is to identify all these experiments in a database that activate the seed region. Subsequently, quantitative meta-analysis is employed to test for convergence across the foci reported in these experiments. As experiments are selected by activation in the seed, the highest convergence will be observed in the seed region itself. Significant convergence of reported foci in other brain regions, however, indicates consistent co-activation, i.e., functional connectivity with the seed (Eickhoff et al. 2010; Robinson et al. 2010). All coordinates used for meta-analysis were expressed in MNI-152 space; where necessary, Talairach coordinates were transformed using methods described in Lancaster et al. (2007).

In this study, we employed the BrainMap database (Laird et al. 2009, 2011) (http://www.brainmap.org). Only those studies that reported group analyses of functional mapping experiments of healthy subjects were included; i.e., all studies that dealt with disease or drug effects were excluded. No further constraints (e.g., on acquisition and analysis details, experimental design, or stimulation procedures) were enforced, yielding approximately 6500 experiments for analysis. Note that we considered all eligible BrainMap experiments because any pre-selection of taxonomic categories would have constituted a fairly strong a priori hypothesis about how brain networks are organized. This was a conservative approach, given that an understanding of how psychological constructs, such as action and cognition, map onto regional brain responses remains elusive (Laird et al. 2009; Poldrack 2006; Poldrack et al. 2011).

To delineate task-based co-activation of the seed region, we first identified all experiments in the BrainMap database that reported group analyses of functional mapping experiments of healthy subjects, and which featured at least one focus of activation in the respective seed. The convergence of foci reported in these experiments was quantified using the revised activation likelihood estimation (ALE) algorithm (Eickhoff et al. 2010) for coordinate-based meta-analysis of neuroimaging results (Eickhoff et al. 2009; Laird et al. 2009; Turkeltaub et al. 2002) implemented as in-house MATLAB tools (Fig. 1d). This algorithm aims to identify areas showing a higher degree of convergence of reported coordinates across experiments than is expected from a random spatial association. Reported foci are not treated as single points, but rather as centers for 3D Gaussian probability distributions capturing the spatial uncertainty associated with each focus. The probabilities of all foci reported in a given experiment are then combined for each voxel, resulting in a modeled activation (MA) map (Eickhoff and Grefkes 2011; Turkeltaub et al. 2012). Taking the union across these MA maps yielded voxel-wise ALE scores describing the convergence of results at each

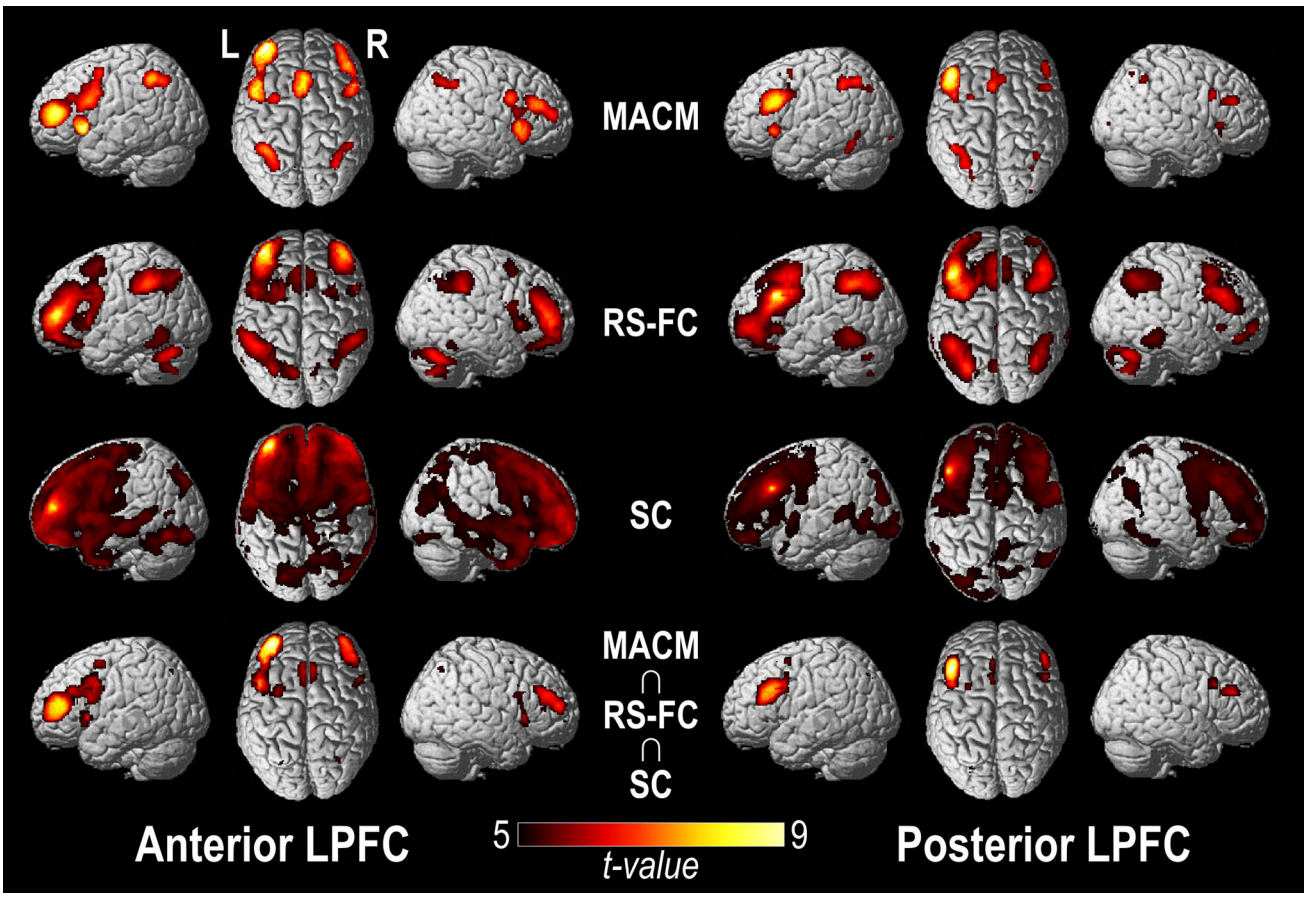

Fig. 2 Brain-wide distribution of connectivity inferred from four imaging methods, using the left aLPFC and pLPFC as seed regions. *MACM* meta-analytic task-based co-activation, *RS-FC* task-independent resting-state BOLD functional connectivity. *SC* structural covariance of gray matter volume, estimated with voxel-based morphometry (VBM). *MACM* ∩ *SC* ∩ *RS-FC* minimum-statistic conjunction across all three approaches. All analyses were performed in MNI space

particular location of the brain. To distinguish 'true' convergence between studies from random convergence (i.e., noise), ALE scores were compared to a null distribution reflecting a random spatial association between experiments (Eickhoff et al. 2012). Hereby, a random-effects inference was invoked, focussing on the above-chance convergence between studies, rather than clustering foci within a particular study. Additionally, to correct for potential over-representation in the literature of activation in the networks of interest, the SCALE approach to MACM was used (Langner et al. 2014). The p value of a "true" ALE was then given by the proportion of equal or higher values obtained under the null distribution, and the resulting non-parametric p values for each meta-analysis were thresholded at a cluster-level corrected threshold of $p < 0.05$ (cluster-forming threshold at voxel-level $p < 0.001$) and transformed into t values for display (Fig. 2). For the current study, we used 188 studies, totalling 1,126 experiments and 12,132 foci (see Supporting Information for corresponding BrainMap Sleuth workspace file).

Resting-state fMRI functional connectivity

Resting-state fMRI images of 207 healthy volunteers (mean age 46.6 ± 16.7 years; 135 females) from the Enhanced NKI/Rockland sample (Nooner et al. 2012) were obtained through the 1000 Functional Connectomes Project (http://www.nitrc.org/projects/fcon_1000/). Data collection received ethics approval through both the Nathan Klein Institute and Montclair State University, and written informed consent was obtained from all participants before data collection. Our use of this publicly available dataset was also approved by the by the local Ethics Committee of the Faculty of Medicine, Heinrich Heine University, Düsseldorf. Written informed consent was obtained from all participants. During the resting state scans subjects were instructed to keep their eyes closed and to think about nothing in particular but not to fall asleep (which was confirmed by post-scan debriefing). For each subject 260 resting state EPI images were acquired on a Siemens TimTrio 3T scanner using blood-oxygen-level-dependent

(BOLD) contrast [gradient-echo EPI pulse sequence, TR = 2.5 s, TE = 30 ms, flip angle = 80°, in plane resolution = 3.0 × 3.0 mm^2, 38 axial slices (3.0 mm thickness) covering the entire brain]. The first four scans were excluded from further processing analysis using SPM8. The EPI images were first corrected for movement artifacts by affine registration using a two-pass procedure in which the images were first aligned to the initial volumes and subsequently to the mean after the first pass. The obtained mean EPI of each subject was then spatially normalized to the MNI single-subject template using the 'unified segmentation' approach (Ashburner and Friston 2000). The ensuing deformation was applied to all individual EPI volumes. To improve signal-to-noise ratio and compensate for residual anatomical variations, images were smoothed by a 5-mm FWHM Gaussian.

The time-series data of each voxel were processed as follows (Eickhoff et al. 2011; Fox et al. 2009; Jakobs et al. 2012; Weissenbacher et al. 2009; Zu Eulenburg et al. 2012): in order to reduce spurious correlations, variance that could be explained by the following nuisance variables was removed—(a) the six motion parameters derived from the image realignment; (b) the first derivative of the realignment parameters; (c) mean gray matter, white matter, and CSF signal per time-point as obtained by averaging across voxels attributed to the respective tissue class in the SPM8 segmentation; and (d) coherent signal changes across the whole brain as reflected by the first five components of a principal component analysis (PCA) decomposition of the whole-brain time series (PrinCor denoising). Age and sex were also considered nuisance variables. All nuisance variables entered the model as first- and (apart from the PCA components) second-order terms as previously described by Behzadi et al. (2007) and shown by Chai et al. (2012) to increase specificity and sensitivity of the analyses. Data were then band-pass filtered to preserve only frequencies between 0.01 and 0.08 Hz, since meaningful resting state correlations will predominantly be found in these frequencies given that the bold-response acts as a low-pass filter (Biswal et al. 1995; Fox and Raichle 2007; Greicius et al. 2003).

For each subject, time series were extracted for all voxels within the aLPFC and pLPFC seed regions and expressed as their first eigenvariate. Using SPM, general linear models were then computed to analyze the degree of association between both seed regions and all other gray matter voxels in the brain. This yielded a measure of resting-state functional connectivity (Zu Eulenburg et al. 2012). Voxel-wise beta coefficients were then transformed into Fisher's *Z*-scores and tested for consistency across subjects in a random-effects analysis. We considered both positive and negative effects. For positive effects, we computed both the main effect for each seed region, and contrasts of aLPFC–pLPFC and pLPFC–aLPFC; i.e., quantifying where the effect of one region was significantly greater than the other. For negative effects, to characterize the antagonistic relationships of aLPFC and pLPFC, we performed a conjunction analysis between voxels anticorrelated with these seed regions and voxels comprising the DMN as defined meta-analytically by Schilbach et al. (2012). Similarly, because emotional processes are hypothesized to have a detrimental effect on WM and attention (Dolcos et al. 2013), we performed a second conjunction analysis between anticorrelated voxels and an emotional processing network (EMO), defined in the same article. In all cases, the statistical maps were thresholded at $p < 0.05$, cluster-level corrected for family-wise error (FWE).

Structural covariance

Structural covariance (SC) measures the degree to which the morphology (i.e., volume, density, or thickness) of brain tissue covaries across a population (Alexander-Bloch et al. 2013; Evans 2013; Reid and Evans 2013). This covariance can be due to a number of influences, one of which may be the effect of common trophic influences induced by the underlying anatomical network structure. Thus, SC has been used to infer a normative (population-based) connectivity structure in a growing number of neuroimaging studies. In order to investigate the brain-wide pattern of structural covariance with the left aLPFC and pLPFC seeds, we used the anatomical T1-weighted images from the same subjects as described above for the RS-FC analysis. These images were acquired on a Siemens TimTrio 3T scanner using an MP-RAGE sequence (TR = 2.5 s, TE = 3.5 ms, TI = 1200 ms, flip angle = 8°, FOV = 256 mm, 192 slices, voxel size 1 × 1 × 1 mm). The anatomical scans were preprocessed using the VBM8 toolbox (dbm.neuro.uni-jena.de/vbm) in SPM8 using standard settings (DARTEL normalization, spatially adaptive non-linear means denoising, a Markov random field weighting of 0.15 and bias field modeling with a regularization term of 0.0001 and a 60 mm FWHM cut-off). The resulting normalized gray matter segments, modulated only for the non-linear components of the deformations into standard space, were smoothed using an 8-mm isotropic FWHM kernel and statistically analyzed by non-parametrical statistics using the "permute" function in FSL. In particular, we first computed the volume of the seed region by integrating the modulated voxel-wise gray matter probabilities for each subject. This vector of subject-specific local volumes represented the covariate of interest in the voxel-wise SPM analysis, and age and sex were included as nuisance variables. Total brain volume was not included in this analysis, as the modulated gray

matter probability maps consist only of local, non-linear deformations. Statistical significance was evaluated at $p < 0.05$, and corrected for multiple comparisons using full permutation testing of threshold-free cluster enhancement (TFCE) images (Smith and Nichols 2009), as implemented in SPM.

Convergence across modalities

The three imaging modalities considered here (MACM, RS-FC, and SC) have substantial conceptual and methodological differences. To assess the degree of convergence between them, we performed a conjunction analysis using the minimum statistics approach (Jakobs et al. 2012; Nichols et al. 2005). We aimed at identifying voxels that showed consistent covariance by computing the intersection of the (cluster-level FWE corrected) thresholded connectivity maps of each pair of analyses, as well as all three together. That is, only voxels with suprathreshold statistics in all maps were included in the resulting conjunction. Given the putative roles of aLPFC and pLPFC in WM processes, we were further interested in determining whether the connectivity of these regions overlapped with the two components of the WM network determined in Rottschy et al. (2012). Accordingly, we computed additional conjunctions between the three modalities and: (a) the task-set network; and (b) both task-set and task-load networks. These latter conjunctions allow us to characterize the extent of the "core" seed-related networks involved in WM processing.

Results

Note: for all analyses, closer inspection of the results is possible by obtaining and viewing the NIFTI images, provided as downloadable Supplemental Material.

MACM co-activations

Left aLPFC showed bilateral, task-dependent co-activation with pLPFC, anterior insula, Broca's region, posterior IFG and posterior SFG as well as with medial (pre-)supplementary motor area [(pre-) SMA; Fig. 2]. Co-activation was also found in bilateral basal ganglia, especially in the nucleus caudatus and thalamus, as well as in the intraparietal sulcus (IPS; areas hIP1-3) and the inferior parietal cortex (IPC; areas PFm, PGa). Left pLPFC showed co-activation with aLPFC and pLPFC bilaterally, left paracingulate gyrus, bilateral superior lateral occipital cortex (LOC) and angular gyrus, left posterior inferior temporal gyrus (ITG), left inferior frontal gyrus (IFG) pars triangularis, and left occipital pole.

Resting-state fMRI correlations

In the RS-FC analysis, aLPFC showed functional connectivity with bilateral pLPFC, ventrolateral PFC, anterior insula, posterior SFG, (pre-) SMA, and the nucleus caudatus (Fig. 2). Bilateral connectivity was also found in the IPS (areas hIP1-3), the IPC (areas PFm, PGa), the superior parietal lobe (areas 7A, 7P), the posterior and middle cingulum, and the cerebellum (Lobule VIIa Crus I, Lobule VI). Connectivity was observed in the left hemisphere only, for: Broca's area, the posterior IFG, the hippocampus, and the entorhinal cortex; and in the right hemisphere only, for: ITG, the retrosplenial cortex, and the aLPFC. Posterior LPFC showed a very similar pattern, indicating a robust co-activation pattern common to both parts of LPFC. However, as shown in Fig. 3, a contrast between seed regions produced two distinct bilateral networks, with aLPFC being more strongly associated with the supramarginal gyrus (SMG), left Broca's area and its homologue, bilateral orbitofrontal cortex, insular cortex, and cerebellum. Posterior

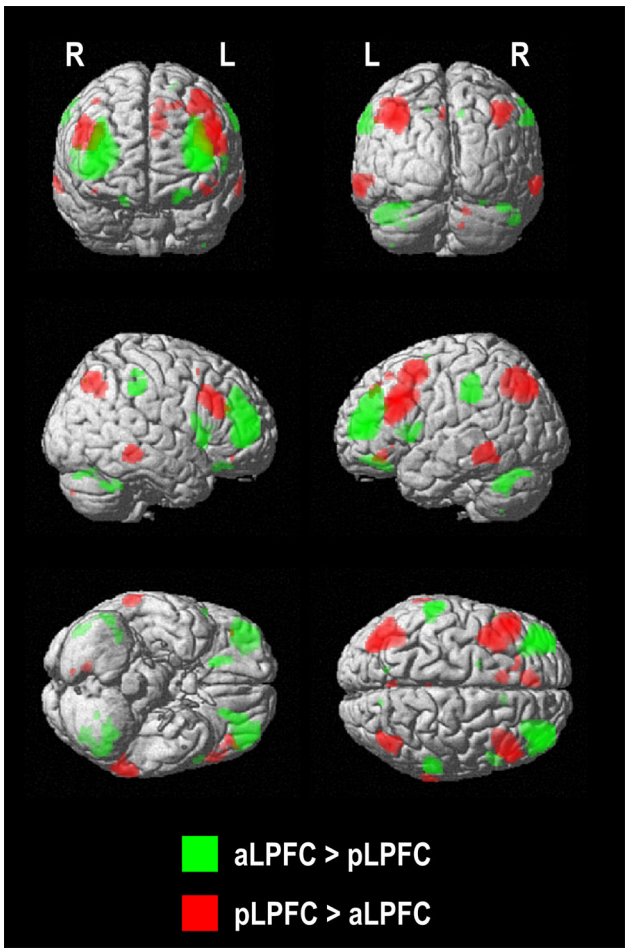

Fig. 3 Contrast between aLPFC and pLPFC RS-fMRI activation, showing regions where the effect of aLPFC was greater than pLPFC (*green*), and vice versa (*red*). Analysis was performed in MNI space

LPFC, on the other hand, was more strongly associated with superior LOC and posterior middle temporal gyrus (MTG) bilaterally, as well as a small region in left paracingulate gyrus.

Structural covariance

Structural covariance (SC) with the left aLPFC was widespread, covering most of lateral and medial frontal cortex (Fig. 2). The SC pattern also included bilateral medial parietal lobe, primarily left lateral parietal lobe, bilateral LOC and ITG, bilateral anterior middle temporal gyrus (MTG), left anterior insula, and right caudate nucleus. For pLPFC, the pattern of SC was generally sparser than for aLPFC, after statistical thresholding. As for aLPFC, SC was most extensive in lateral and medial frontal cortex, with some covariance also evident bilateral in LOC, ITG, and occipitotemporal gyrus.

Convergence across modalities

All three modalities (MACM, RS-fMRI, and SC) revealed similar patterns of left aLPFC associations across the cortex, although these differed markedly in extent. The significant conjunction between these patterns is shown in Fig. 2. It includes both aLPFC and pLPFC, Broca's area (pars opercularis), the anterior insula, paracingulate cortex, Broca's area, superior LOC, IPS (hIP1-3), IPC (PGa) and (pre-) SMA. This pattern occurred bilaterally, but was more prominent in the left than right hemisphere. Subcortical connectivity was furthermore revealed in the left caudate nucleus. For left pLPFC, this pattern was sparser, including pLPFC bilaterally, left paracingulate cortex, left superior LOC, and a small region of Broca's area (pars triangularis).

Conjunction with WM networks

To assess the degree to which the aLPFC-seed networks overlap with those involved in WM, a further conjunction analysis was conducted between the cross-modal conjunction, described above, and the coordinate-based task-set WM network reported previously in Rottschy et al. (2012; Fig. 4). This network included: bilateral anterior LPFC, Broca's region, anterior insula, posterior SFG, paracingulate cortex, (pre-) SMA, IPS (areas hIP1-3), and SPL (areas 7PC, 7A); as well as the left basal ganglia subcortically (particularly, thalamus and nucleus caudatus). For aLPFC, the resulting conjunction, while substantially sparser, included nearly all regions of the task-set network, with the exception of superior parietal cortex (intersection = 17.4 %). Posterior LPFC, which was even sparser, overlapped only for pLPFC bilaterally, and left paracingulate gyrus (intersection = 7.6 %). An additional comparison was performed between the joint task-set and task-load conjunction, reported in the same study, and the cross-modal conjunction (21.7 % for aLPFC and 14.6 % for pLPFC). This resulted in a nearly identical set of regions as for the task-set only conjunction, for both seed regions.

Resting-state fMRI anticorrelations

Areas which were anticorrelated with the aLPFC for RS-fMRI time series comprised a widespread network covering the medial surface of the frontal and parietal lobes as well as the anterior and posterior cingulate cortex, the lateral and medial temporal lobes (including the amygdala), the primary sensory motor cortex, the parietal operculum and a large region in the temporal parietal occipital junction as well as parts of the cerebellum (Fig. 5). For pLPFC, anti-correlations were also quite widespread, comprising medial and lateral occipital cortex, cuneus, lingual gyrus, anterior precuneus, middle and anterior cingulate gyrus, temporo-occipital fusiform gyrus, superior parietal lobule, hippocampus, and cerebellum. A conjunction analysis across this network and regions anticorrelated with the left aLPFC in the present study, resulted in nearly all regions of the DMN being retained (overlap = 28.1 %)—supporting the hypothesis that the DMN is anticorrelated with WM tasks. Augmenting this finding, a further conjunction analysis between the combined DMN/EMO networks and aLPFC anticorrelations resulting in a near identical distribution (overlap = 8.6 %). For pLPFC, a much smaller overlap was found with the DMN (8.6 %), apart from right temporoparietal junction, and small regions of LOC, precuneus, posterior parietal cortex, and inferior paracingulate gyrus. It had no overlap with the DMN/EMO network.

Discussion

Summary of findings

In a previous coordinate-based meta-analysis of functional neuroimaging studies (Rottschy et al. 2012), we found a consistent involvement of the left aLPFC in WM tasks (contrast between a WM task and a non-WM control) per se, and an involvement of pLPFC in contrasts for task load, supporting a functional differentiation of the two areas. Here, we further investigated the left aLPFC and pLPFC in order to characterize their connectivity profiles across three imaging modalities (task-negative RS-FC, task-positive MACM, and SC). All three modalities yielded connectivity patterns that were

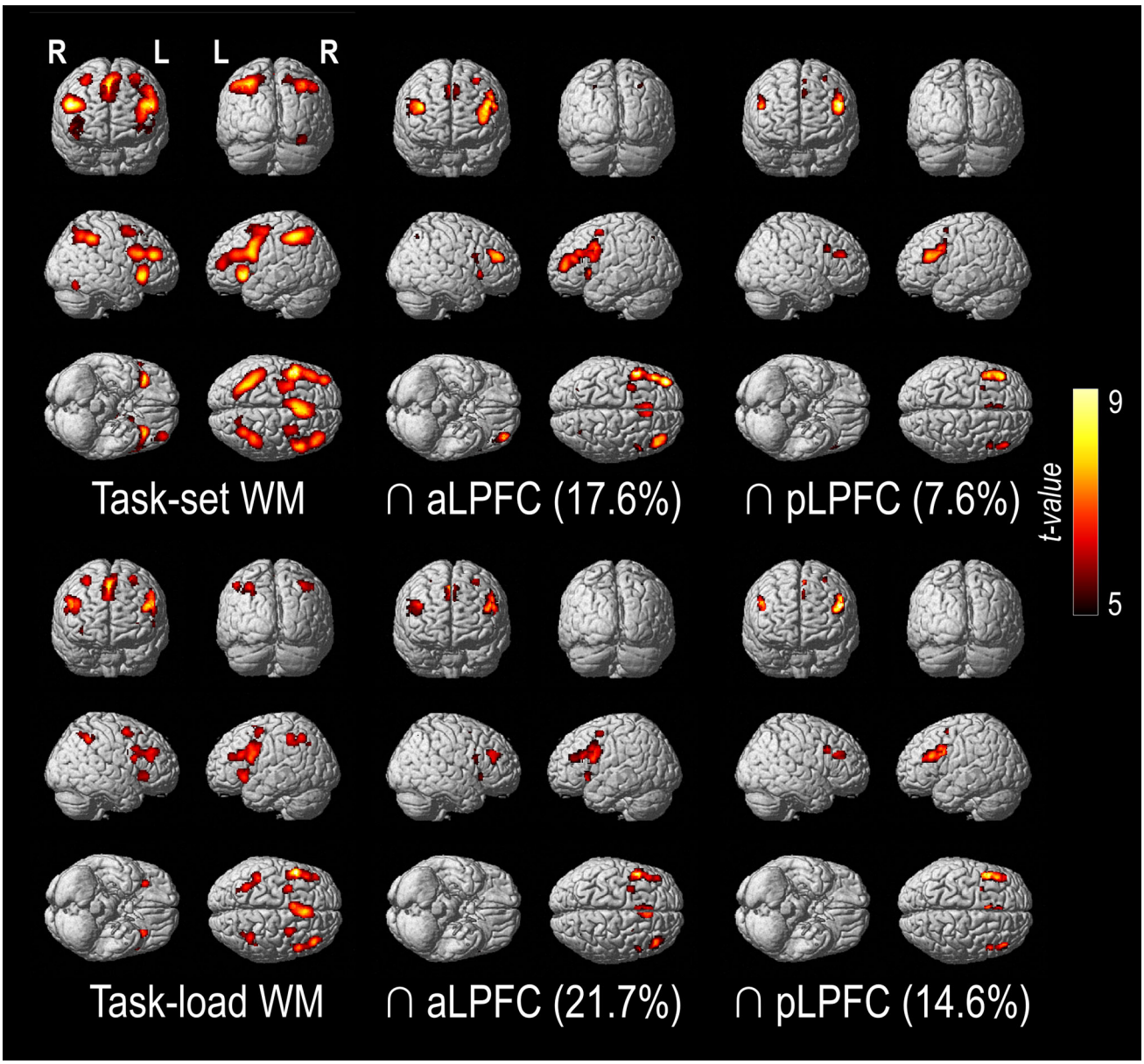

Fig. 4 Comparison of aLPFC and pLPFC connectivity to the working memory (WM) networks reported in Rottschy et al. (2012). *Top* the task-set network is an ALE distribution of studies contrasting WM task with a baseline or other control condition. At right, a conjunction of the task-set network with the cross-modal conjunctions shown in Fig. 2. *Bottom* a conjunction of the task-set network and a second ALE analysis contrasting high- and low-load WM task conditions (task-load network). The distribution resembles a reduced version of the task-set network. At *right*, a conjunction of the task-load network with the cross-modal conjunctions for aLPFC and pLPFC. These regions constitute a "core" WM-related network. *Labels* show percent intersection. All analyses were performed in MNI space

qualitatively similar, with SC having the greatest extent and MACM the least. We found a strong conjunction between these patterns and both of the previously identified task-set and task-load WM networks, with the exception of Broca's area and the IFG. Furthermore, for the RS-FC approach, we found distinct set of regions when contrasting aLPFC and pLPFC effects, with the former more strongly associated with cortical regions thought to subserve higher-level functions (SMG, Broca's area, and insula) and the latter more strongly associated with lower-level regions (superior LOC and posterior MTG). Finally, we found a widespread pattern of regions anticorrelated with both aLPFC and pLPFC activation, with only the former having a substantial overlap with most of the DMN and joint DMN/EMO networks identified by Schilbach et al. (2008).

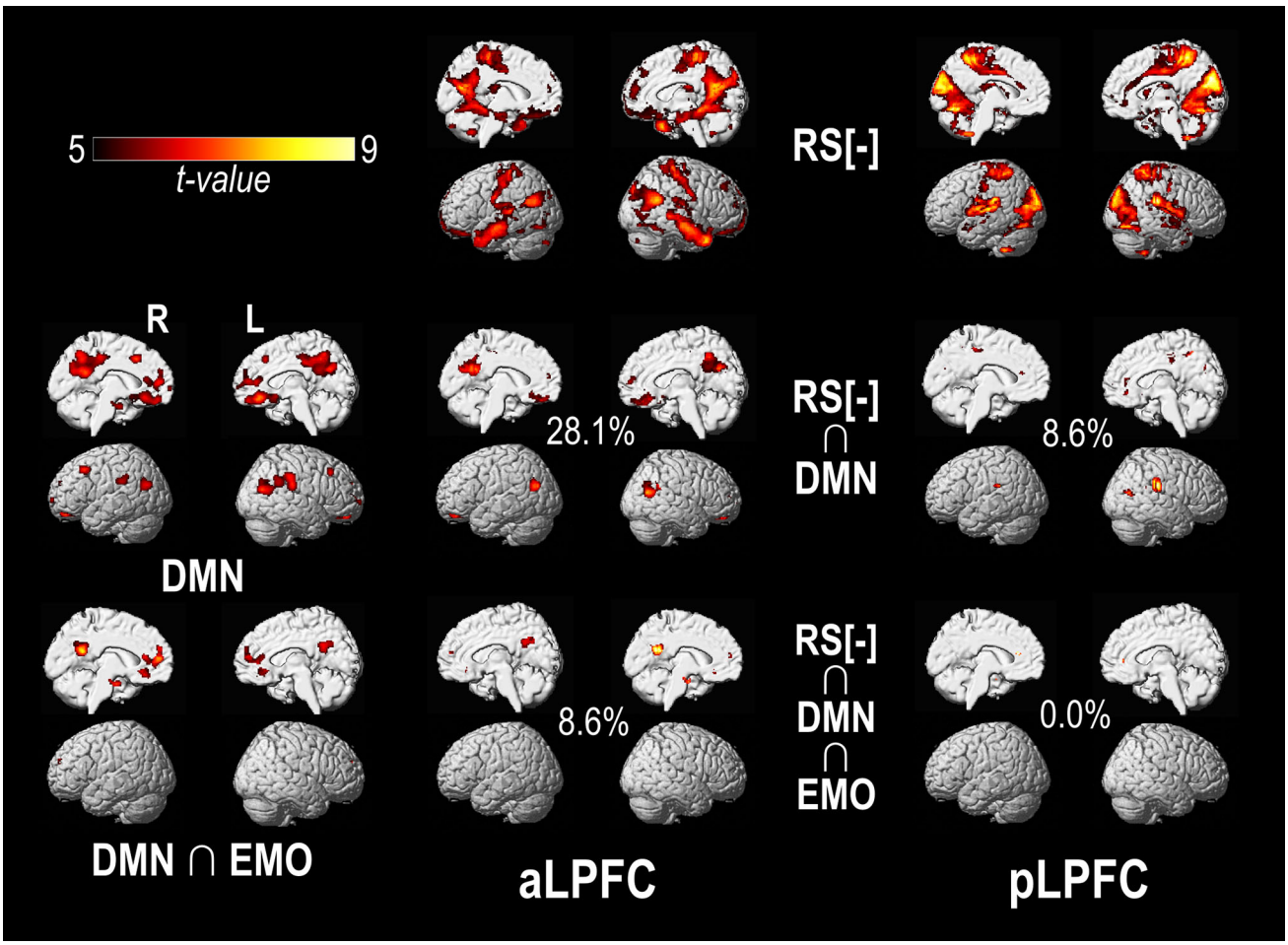

Fig. 5 *Top row* RS-fMRI anticorrelations (RS[−]) for the aLPFC and pLPFC seeds, which imply an antagonistic relationship across much of cortex. *Second row* The default mode network (DMN) defined by Schilbach et al. (2012), and a conjunction of this with the RS[−] network with aLPFC and pLPFC. *Bottom row* A conjunction of the DMN with an ALE distribution of studies contrasting emotional processing with a control condition. The regions are all medial, and consist of PCC, dorsal ACC, mPFC, and amygdala. At *right*, a conjunction of this network with the aLPFC RS[−] network is nearly identical to it, while there is virtually no overlap with the pLPFC network. All analyses were performed in MNI space

Role of the frontoparietal network in working memory

The LPFC has long been characterized as a core part of Baddeley and Hitch's central executive module (Baddeley 2000, 2003; Baddeley and Hitch 1974), and fMRI evidence suggests it plays a critical role in the coordination and selection of WM processes (Barch et al. 1997; Braver et al. 2001). The meta-analytic findings of Rottschy et al. (2012) suggest a further differentiation of LPFC into anterior and posterior parts, with the aLPFC being associated with the setting and selection of WM tasks and pLPFC being associated with differences in task difficulty. Our present results demonstrate that, across both overt tasks and resting state, the aLPFC shows both co-activation and structural covariance with task-set and task-load networks, while the pLPFC overlaps to a lesser extent. This multimodal evidence is in line with the proposed role of aLPFC as a "hub" region which coordinates WM processes; a role that is likely implemented through modulation of the activity of more posterior regions, including posterior parietal and temporo-occipital cortices, which actually store volatile information. This organization also corresponds to the hypothesized anterior (overarching planning) to posterior (lower-level execution) axis of the prefrontal cortex in executive control (Badre 2008; Koechlin and Summerfield 2007). It is further substantiated by EEG evidence that theta-band coherence between LPFC and parietal regions is increased when subjects perform WM tasks (Sarnthein et al. 1998; Sauseng et al. 2005), and also visuospatial tasks involving novel, but not memorized, motor sequences (Sauseng et al. 2007). It is, however, important to note that the task-set and task-load networks derived previously correspond to a wide array of paradigms, which allows for

alternative interpretations of these networks. As previously noted in Rottschy et al. (2012), the task-set condition includes the possible confounds of altered arousal, attention, and response selection. However, as is argued here, these components are likely inherent to WM itself, and therefore not separable from it (see also the discussion of internal attention models, below). For the task-load condition, the possibility that subjects are recruiting alternative cognitive strategies (e.g., "chunking") to perform harder WM tasks should also be taken into consideration. Thus, the co-activation patterns which correspond to the task-load network likely include a mixture of distinct or interacting neural responses to increased WM load, rather than representing a single stereotypical response profile (see review by Stuss, 2006).

Several lines of evidence support a tight overlap between the concepts of selective attention and WM (reviewed in Gazzaley and Nobre 2012), which fit the present results. For instance, the LPFC networks shown in Fig. 4 are similar to the multiple-demand *system* (Duncan 2010), which includes IFS, anterior insula, pre-SMA, dorsal ACC, and IPS. The multiple-demand network has been proposed to subserve the control and planning of diverse cognitive tasks, and is associated with fluid intelligence and problem solving. Duncan (2013) suggests that the fundamental role of this network is as an attentional system, coordinating the allocation of cognitive resources on the basis of "demand". The dorsal attention network (DAN) comprises a very similar set of regions, which include the FEF/PMC and IPS/SPL (reviewed in Lückmann et al. 2014). Corbetta and colleagues have proposed that the human attentional system comprised anatomically and functionally distinct dorsal and ventral components, with the former specialized for linking perceptual input to adaptive behavior, and the latter allowing reorientation to salient external stimuli (Corbetta et al. 2008). The DAN has been also proposed by Lückmann and colleagues as subserving an overarching control mechanism consistent with activation patterns in WM, long-term memory consolidation, and visual imagery. These authors propose that these cognitive paradigms, despite having distinct psychological definitions, each rely on internal attention, as implemented by the DAN. In this model, internal attention acts to modulate "reverberating perceptual activation" in sensory and perceptual circuits in the absence of exogenous input, depending on the material of the specific task. In line with this theory, theta-band coherence between frontal and parietal regions was related to performance of both attentional (Makeig et al. 2004) and WM (Deiber et al. 2007; Gomarus et al. 2006) tasks. Theta modulation has been proposed as a general mechanism for enhancing spike-based connectivity between brain regions (Lisman 2005), and may represent the neurophysiological mechanism through which the LPFC-associated network subserves WM.

Hierarchical models of cognitive control in the LPFC

Apart from WM, a more general framework for the function of the LPFC is that of cognitive control (reviewed in Badre 2008). Most theories of cognitive control conceptualize it as a hierarchical system, in which activity in higher-level regions, implementing more abstract representations of objects and actions, modulates activity in lower-level regions, implementing more concrete representations of sensory input or motor output. As with attentional processes, top-down cognitive control allows the system to bias competing lower-level representations according to the expectations, goals, and contextual information they contain (Duncan 2001, 2013; Koechlin and Summerfield 2007). This hierarchical model of LPFC function has also been proposed to feature an anteroposterior gradient, with anterior LPFC representing increasingly abstract and temporally sustained information, and posterior LPFC representing increasingly concrete (sensorimotor) and temporally proximal information. This organization has been substantiated by multiple lines of evidence, including an investigation of patients with frontal lesions (Badre et al. 2009). Koechlin et al. (2003), based on a task-based fMRI paradigm, have proposed a "cascade model" of cognitive control, in which processing of past events (episodic), current context (contextual), and current stimuli (sensory) corresponded to aLPFC, pLPFC, and PMC, respectively.

It is important to emphasize that the present evidence does not directly substantiate the role of the LPFC as a WM or cognitive control hub, due to the limitations of reverse inference (see Poldrack 2006). However, it is useful to observe that the present results are consistent with this role, in particular with respect to the differential co-activation patterns corresponding to its anterior and posterior subdivisions. In particular, the contrast between aLPFC and pLPFC RS-fMRI effects demonstrates a clear separation between the connectivity patterns of these subregions. Furthermore, as predicted by the theory that the anteroposterior axis of the LPFC represents a hierarchical functional continuum from abstract to concrete representations, we find that aLPFC is most strongly associated with higher-level areas, including SMG, Broca's area, orbitofrontal cortex, and anterior insula. The former two are likely critical regions for verbal WM (Deschamps et al. 2014; Rogalsky et al. 2008); that is, they have been proposed to constitute the phonological loop component of the Baddeley model. Lesions of the orbitofrontal cortex disrupt the coordination, monitoring, and manipulation of WM content, but not its maintenance (Barbey et al. 2011). We would argue that this observation supports the role of aLPFC as a higher-level coordinator of cognitive processes

(including, but likely not exclusive to, WM). In contrast, pLPFC was most strongly associated with activity in superior LOC and posterior MTG. These regions both occupy intermediate positions in the visual processing hierarchy (reviewed in Schenk and McIntosh 2010), and therefore represent more concrete perceptual representations of visual stimuli. Their stronger functional association with pLPFC is thus also consistent with the hierarchical anteroposterior organization of the LPFC.

aLPFC, but not pLPFC, is anticorrelated with DMN and EMO

For resting-state fMRI, we also found a substantial degree of activity which was anticorrelated with the left aLPFC seed region, and this pattern included most of the DMN and joint DMN/EMO networks defined in Schilbach et al. (2012). Additionally, the MACM results showed no co-activation between the aLPFC and these networks. Notably, a similar overlap was not found for pLPFC, with the exception of right temporoparietal junction. This pattern agrees with numerous reports in the literature. Fox et al. (2005), for instance, have reported BOLD activations in a network largely resembling the DMN, which is generally activated in the absence of overt task demands, and was accordingly named the task-negative network. Similarly, in an earlier PET study, Drevets and Raichle (1998) reported increases in DLPFC and dorsal ACC during attention-demanding cognitive tasks, but a corresponding decrease in amygdala, posteromedial orbital cortex, and ventral ACC, which agrees with the conjunction between anticorrelations and the joint DMN/EMO network reported here (see Fig. 5). The authors further relate this dichotomy to an antagonism between emotional states and cognitive performance, and the ACC in particular has been functionally partitioned on the basis of this antagonistic relationship (Mohanty et al. 2007). These findings lend support for the hypothesis that WM is in essence an internal attentional process, controlling activity in "buffers" by modulating their activity—that is, acting as a top-down control system which selects the sequence of processing and information transfer required for a WM task (Duncan 2010; Gazzaley and Nobre 2012; Lückmann et al. 2014). DMN- and EMO-related thought processes have been proposed to interfere with this function by diverting attentional resources away from the task-positive (aLPFC-associated) network and towards the task-negative (DMN/EMO) one (Dolcos et al. 2013).

Cross-modal comparisons

We have defined "core network" as the extent of connectivity results that survive statistical thresholding across all three modalities (the so-called minimum-statistic approach, cf. Nichols et al. 2005). This is a highly conservative approach, which identifies a network for which there is full agreement (in other words, convergence) across modalities. Thus, a core network in this sense refers to a set of brain regions with statistically significant relationships to the seed region about which we have a high level of confidence. It is not, on the other hand, meant to suggest that these regions constitute the full core network in a functional sense. Different modalities may capture distinct aspects of inter-regional associations which are not detected by the others, and thus provide complementary information. Indeed, such modality specificity was observed in our study. The nature of the disagreement would also be a useful consideration (cf., Clos et al. 2014), but at present the separation of methods-specific bias from methods-specific (true) findings remains a difficult prospect. In turn, however, we would argue that the conjunction network should be robust to false positive findings, potentially at the expense of somewhat lower power to detect true effects.

In the present study, a number of differences were found between connectivity patterns generated by each modality. The SC network, for instance, had a substantially larger extent than either RS-FC or MACM, particularly in the prefrontal lobe. This approach, based upon across-subject covariance in anatomical morphology, is clearly different than the two fMRI-based methods, which obtain averaged within-subject BOLD signal covariance or contrasts. While correlations in morphology may reflect mutual trophic influences—accumulated over the lifetime of the subject—due to direct or indirect connectivity (Alexander-Bloch et al. 2013; Evans 2013), they likely also reflect the inherent smoothness and symmetry of gray matter tissue, as well as the influence of common genetic factors (Eyler et al. 2012; Wright et al. 2002). While the fMRI-related patterns more closely resembled one another, they also differed in several respects. This variability is attributable in part to the different methodological approaches and inherent sources of noise associated with each technique. RS networks are characterized by spontaneous, task-free fluctuations in the BOLD signal that may be particularly susceptible to artifacts from preprocessing and physiological noise (Chang and Glover 2009). MACM is based upon the convergence of BOLD co-activity between task-based experiments, and is thus biased by the paradigms from which it is derived, and the inherent spatial uncertainty of neuroimaging results (Eickhoff et al. 2009; Rottschy et al. 2012). Given these qualitative and methodological disparities, the observed differences between modalities are not surprising. However, determining where these patterns converge allows us to identify the "core" network for which evidence from all modalities is in agreement.

Methodological limitations

In this analysis we use three diverging connectivity modalities, and report "core" networks representing the overlap of connectivity inferences drawn from each modality. It is important to acknowledge the different limitations inherent in each approach. For instance, because MACM draws information from a large number of independent task-based fMRI studies, it is subject to spatial uncertainty both inherent in the BOLD signal, and due to the sparseness of peak activations across studies. This uncertainty is modeled, however, as Gaussian distributions around each point, and taken into consideration in the statistical analysis. Additionally, MACM utilizes data from the BrainMap database, which also includes some of the experiments that were included in the analysis that defined the seed regions (Rottschy et al. 2012). Importantly, however, this overlap is very minor. Only 21 experiments (i.e., around 10 % of the overall sample) were part of both the MACM and the WM meta-analysis. This also highlights the key feature of MACM, i.e., that it draws from all eligible data across paradigms and hence represents a location rather than function-centered view on (co-) activation patterns. When considering the RS-fMRI functional connectivity analysis, it may be noted that we first regressed out the mean signal in white, gray, and CSF tissue, a form of global signal regression (GSR). GSR has been argued to induce spurious anti-correlations in fMRI data (Murphy et al. 2009), and the interpretation of such anti-correlations is still an open debate, with some evidence that they represent biologically valid signal (Fox et al. 2009; Smith et al. 2012). The present anti-correlation results should be considered in the context of this issue. Finally, it bears consideration that inferences about connectivity are based upon correlational evidence, in the case of RS-fMRI and SC, and coincidence, in the case of MACM; such statistical dependence could reflect either direct or indirect structural connectivity (for review, see Friston 2011). However, convergence of evidence across multiple modalities, as presented here, provides a stronger basis upon which to infer the existence of a brain network, as such approach should be less subject to the limitations and biases of each method individually.

Additional neuroimaging modalities have been used to infer different aspects of connectivity, which have not been used in the present study. While the addition of a new modality allows more complementary information to be used in identifying a core network, each addition also introduces another set of limitations, which on aggregate lowers the extent to which all modalities agree. Thus, in the present study we chose to limit the modalities to the three chosen. However, a few additional approaches might be addressed in future studies. Firstly, for the VBM approach, estimates of brain morphology are volumetric, and thus fail to some extent to measure the gyral morphology of the cortical sheet, as is available via surface-based methods such as Freesurfer (Dale et al. 1999), CIVET (Kim et al. 2005), or CARET (Van Essen 2004). However, these methods are each dependent on universal tissue classification algorithms, which fail to capture local differences in tissue composition, and in particular fail to account for the partial contributions made by myelinated axons, somata, and glia to the measured T1-weighted voxel intensity. Thus, the placement of the boundary used to estimate cortical thickness is subject to its own inherent limitations. Secondly, as the methods considered here do not directly consider white matter anatomy, the use of methods such as diffusion-weighted imaging-based (DWI-based) tractography, or polarized light imaging (PLI) could conceivably be used to provide this complementary information. For the present study, however, we considered this infeasible. PLI results are currently restricted to discrete regions of brain tissue, and thus do not provide the necessary whole-brain coverage. Moreover, these data are only obtainable through painstaking post-mortem extraction, preparation, and imaging methods, which limits both their rate of acquisition and their generalizability. The problem of using PLI data to estimate long-range connectivity also remains poorly addressed at present. DWI-based methods are more promising in this respect; however, at present, use of DWI-based probabilistic tractography suffers from a number of biases, including a non-trivial bias for shorter pathways, and a bias imposed by the unequal anisotropy associated with different fiber pathways (Dauguet et al. 2007; Mukherjee et al. 2008). Current work on addressing these biases holds promise for its future inclusion in multimodal analyses.

Conclusion

Our results provide converging evidence for "core" left aLPFC- and pLPFC-associated networks, across three imaging modalities: meta-analytic task-constrained fMRI, resting-state task-unconstrained fMRI, and structural MRI. The aLPFC and, to a lesser extent, pLPFC networks overlap strongly with task-set and task-load 1WM networks defined by a previous ALE analysis (Rottschy et al. 2012), which corresponds to previous fMRI and EEG findings relating frontoparietal connectivity to WM performance. Contrasting aLPFC and pLPFC connectivity revealed a pattern consistent with the theory that LPFC is hierarchically organized along its anteroposterior axis, such that more anterior regions process increasingly abstract information. Moreover, the aLPFC-associated network in particular has a close resemblance to a number of frontoparietal networks previously described in the literature,

including the multiple-demand system and the DAN. We further show that the aLPFC is anticorrelated with a set of regions which includes the DMN and joint DMN/EMO networks (reported by Schilbach et al. 2012), which likely have an antagonistic relationship with aLPFC-associated regions, reflecting a diversion of attentional resources that can interfere with performance on WM and other cognitive tasks. For pLPFC, anticorrelations coincided only with the temporoparietal junction of the DMN, and not at all with the DMN/EMO network. Our findings fit well with the internal attention theory of WM, in which regions of the DAN interact with the aLPFC to control and manipulate information which is maintained, possibly via the pLPFC, through the activity of lower-level regions, including the IFG, SPG, and IPS.

Acknowledgments This study was supported by the Deutsche Forschungsgemeinschaft (DFG, EI 816/4-1, LA 3071/3-1; EI 816/6-1.), the National Institute of Mental Health (R01-MH074457), the Helmholtz-Portfolio Project on "Supercomputing and Modeling for the Human Brain" and the European Union Seventh Framework Programme (FP7/2007-2013) under grant agreement no. 604102 (Human Brain Project).

References

Alexander-Bloch A, Giedd JN, Bullmore E (2013) Imaging structural co-variance between human brain regions. Nat Rev Neurosci 14:322–336

Amunts K, Schleicher A, Bürgel U, Mohlberg H, Uylings HB, Zilles K (1999) Broca's region revisited: cytoarchitecture and inter-subject variability. J Comp Neurol 412:319–341

Ashburner J, Friston KJ (2000) Voxel-based morphometry–the methods. Neuroimage 11:805–821

Awh E, Jonides J (2001) Overlapping mechanisms of attention and spatial working memory. Trends Cogn Sci 5:119–126

Baddeley A (2000) The episodic buffer: a new component of working memory? Trends Cogn Sci 4:417–423

Baddeley A (2003) Working memory: looking back and looking forward. Nat Rev Neurosci 4:829–839

Baddeley AD, Hitch G (1974) Working memory. In: Gordon HB (ed), Psychology of learning and motivation. Academic Press, pp 47–89

Badre D (2008) Cognitive control, hierarchy, and the rostro-caudal organization of the frontal lobes. Trends Cogn Sci 12:193–200

Badre D, Hoffman J, Cooney JW, D'Esposito M (2009) Hierarchical cognitive control deficits following damage to the human frontal lobe. Nat Neurosci 12:515–522

Barbey AK, Koenigs M, Grafman J (2011) Orbitofrontal contributions to human working memory. Cereb Cortex NY N 1991(21):789–795

Barch DM, Braver TS, Nystrom LE, Forman SD, Noll DC, Cohen JD (1997) Dissociating working memory from task difficulty in human prefrontal cortex. Neuropsychologia 35:1373–1380

Barrett LF, Tugade MM, Engle RW (2004) Individual differences in working memory capacity and dual-process theories of the mind. Psychol Bull 130:553–573

Behzadi Y, Restom K, Liau J, Liu TT (2007) A component based noise correction method (CompCor) for BOLD and perfusion based fMRI. NeuroImage 37:90–101

Berryhill ME, Chein J, Olson IR (2011) At the intersection of attention and memory: The mechanistic role of the posterior parietal lobe in working memory. Neuropsychologia 49:1306–1315

Biswal B, Zerrin Yetkin F, Haughton VM, Hyde JS (1995) Functional connectivity in the motor cortex of resting human brain using echo-planar mri. Magn Reson Med 34:537–541

Braver TS, Barch DM, Kelley WM, Buckner RL, Cohen NJ, Miezin FM, Snyder AZ, Ollinger JM, Akbudak E, Conturo TE, Petersen SE (2001) Direct comparison of prefrontal cortex regions engaged by working and long-term memory tasks. NeuroImage 14:48–59

Buckner RL, Andrews-Hanna JR, Schacter DL (2008) The brain's default network: anatomy, function, and relevance to disease. Ann N Acad Sci 1124:1–38

Caspers S, Geyer S, Schleicher A, Mohlberg H, Amunts K, Zilles K (2006) The human inferior parietal cortex: cytoarchitectonic parcellation and interindividual variability. NeuroImage 33:430–448

Caspers S, Eickhoff SB, Geyer S, Scheperjans F, Mohlberg H, Zilles K, Amunts K (2008) The human inferior parietal lobule in stereotaxic space. Brain Struct Funct 212:481–495

Chai XJ, Castañón AN, Ongür D, Whitfield-Gabrieli S (2012) Anticorrelations in resting state networks without global signal regression. NeuroImage 59:1420–1428

Chang C, Glover GH (2009) Effects of model-based physiological noise correction on default mode network anti-correlations and correlations. NeuroImage 47:1448–1459

Choi H-J, Zilles K, Mohlberg H, Schleicher A, Fink GR, Armstrong E, Amunts K (2006) Cytoarchitectonic identification and probabilistic mapping of two distinct areas within the anterior ventral bank of the human intraparietal sulcus. J Comp Neurol 495:53–69

Christoff K, Gabrieli JDE (2013) The frontopolar cortex and human cognition: evidence for a rostrocaudal hierarchical organization within the human prefrontal cortex. Psychobiology 28:168–186

Christoff K, Ream JM, Geddes LPT, Gabrieli JDE (2003) Evaluating self-generated information: anterior prefrontal contributions to human cognition. Behav Neurosci 117:1161–1168

Clos M, Rottschy C, Laird AR, Fox PT, Eickhoff SB (2014) Comparison of structural covariance with functional connectivity approaches exemplified by an investigation of the left anterior insula. NeuroImage 99:269–280

Corbetta M, Kincade J, Shulman G (2002) Neural systems for visual orienting and their relationships to spatial working memory. J Cogn Neurosci 14:508–523

Corbetta M, Patel G, Shulman GL (2008) The reorienting system of the human brain: from environment to theory of mind. Neuron 58:306–324

D'Esposito M, Postle BR (1999) The dependence of span and delayed-response performance on prefrontal cortex. Neuropsychologia 37:1303–1315

Dale AM, Fischl B, Sereno MI (1999) Cortical surface-based analysis. I. Segmentation and surface reconstruction. Neuroimage 9:179–194

Dauguet J, Peled S, Berezovskii V, Delzescaux T, Warfield SK, Born R, Westin C-F (2007) Comparison of fiber tracts derived from in vivo DTI tractography with 3D histological neural tract tracer reconstruction on a macaque brain. NeuroImage 37:530–538

Deiber M-P, Missonnier P, Bertrand O, Gold G, Fazio-Costa L, Ibañez V, Giannakopoulos P (2007) Distinction between perceptual and attentional processing in working memory tasks:

a study of phase-locked and induced oscillatory brain dynamics. J Cogn Neurosci 19:158–172

Deschamps I, Baum SR, Gracco VL (2014) On the role of the supramarginal gyrus in phonological processing and verbal working memory: Evidence from rTMS studies. Neuropsychologia 53:39–46

Desikan RS, Ségonne F, Fischl B, Quinn BT, Dickerson BC, Blacker D, Buckner RL, Dale AM, Maguire RP, Hyman BT, Albert MS, Killiany RJ (2006) An automated labeling system for subdividing the human cerebral cortex on MRI scans into gyral based regions of interest. NeuroImage 31:968–980

Dolcos F, Iordan AD, Kragel J, Stokes J, Campbell R, McCarthy G, Cabeza R (2013) Neural correlates of opposing effects of emotional distraction on working memory and episodic memory: an event-related FMRI investigation. Front. Psychol. 4:293

Drevets W, Raichle M (1998) Reciprocal suppression of regional cerebral blood flow during emotional versus higher cognitive processes: Implications for interactions between emotion and cognition. Cogn Emot 12:353–385

Du Boisgueheneuc F, Levy R, Volle E, Seassau M, Duffau H, Kinkingnehun S, Samson Y, Zhang S, Dubois B (2006) Functions of the left superior frontal gyrus in humans: a lesion study. Brain 129:3315–3328

Duncan J (2010) The multiple-demand (MD) system of the primate brain: mental programs for intelligent behaviour. Trends Cogn Sci 14:172–179

Duncan J (2013) The structure of cognition: attentional episodes in mind and brain. Neuron 80:35–50

Eickhoff SB, Grefkes C (2011) Approaches for the integrated analysis of structure, function and connectivity of the human brain. Clin EEG Neurosci 42:107–121

Eickhoff S, Walters NB, Schleicher A, Kril J, Egan GF, Zilles K, Watson JDG, Amunts K (2005) High-resolution MRI reflects myeloarchitecture and cytoarchitecture of human cerebral cortex. Hum Brain Mapp 24:206–215

Eickhoff SB, Heim S, Zilles K, Amunts K (2006) Testing anatomically specified hypotheses in functional imaging using cytoarchitectonic maps. NeuroImage 32:570–582

Eickhoff SB, Paus T, Caspers S, Grosbras M-H, Evans AC, Zilles K, Amunts K (2007) Assignment of functional activations to probabilistic cytoarchitectonic areas revisited. NeuroImage 36:511–521

Eickhoff SB, Laird AR, Grefkes C, Wang LE, Zilles K, Fox PT (2009) Coordinate-based activation likelihood estimation meta-analysis of neuroimaging data: a random-effects approach based on empirical estimates of spatial uncertainty. Hum Brain Mapp 30:2907–2926

Eickhoff SB, Jbabdi S, Caspers S, Laird AR, Fox PT, Zilles K, Behrens TEJ (2010) Anatomical and functional connectivity of cytoarchitectonic areas within the human parietal operculum. J Neurosci Off J Soc Neurosci 30:6409–6421

Eickhoff SB, Bzdok D, Laird AR, Roski C, Caspers S, Zilles K, Fox PT (2011) Co-activation patterns distinguish cortical modules, their connectivity and functional differentiation. NeuroImage 57:938–949

Eickhoff SB, Bzdok D, Laird AR, Kurth F, Fox PT (2012) Activation likelihood estimation meta-analysis revisited. NeuroImage 59:2349–2361

Evans AC (2013) Networks of anatomical covariance. NeuroImage 80:489–504

Eyler LT, Chen C-H, Panizzon MS, Fennema-Notestine C, Neale MC, Jak A, Jernigan TL, Fischl B, Franz CE, Lyons MJ, Grant M, Prom-Wormley E, Seidman LJ, Tsuang MT, Fiecas MJA, Dale AM, Kremen WS (2012) A comparison of heritability maps of cortical surface area and thickness and the influence of adjustment for whole brain measures: a magnetic resonance imaging twin study. Twin Res. Hum. Genet Off J Int Soc Twin Stud 15:304–314

Fletcher PC, Henson RN (2001) Frontal lobes and human memory: insights from functional neuroimaging. Brain J Neurol 124:849–881

Fox MD, Raichle ME (2007) Spontaneous fluctuations in brain activity observed with functional magnetic resonance imaging. Nat Rev Neurosci 8:700–711

Fox MD, Snyder AZ, Vincent JL, Corbetta M, Essen DCV, Raichle ME (2005) The human brain is intrinsically organized into dynamic, anticorrelated functional networks. Proc Natl Acad Sci USA 102:9673–9678

Fox MD, Zhang D, Snyder AZ, Raichle ME (2009) The global signal and observed anticorrelated resting state brain networks. J Neurophysiol 101:3270–3283

Friston KJ (2011) Functional and effective connectivity: a review. Brain Connect 1:13–36

Gazzaley A, Nobre AC (2012) Top-down modulation: bridging selective attention and working memory. Trends Cogn Sci 16:129–135

Gomarus HK, Althaus M, Wijers AA, Minderaa RB (2006) The effects of memory load and stimulus relevance on the EEG during a visual selective memory search task: an ERP and ERD/ERS study. Clin Neurophysiol Off J Int Fed Clin Neurophysiol 117:871–884

Greicius MD, Krasnow B, Reiss AL, Menon V (2003) Functional connectivity in the resting brain: a network analysis of the default mode hypothesis. Proc Natl Acad Sci USA 100:253–258

Hamidi M, Tononi G, Postle BR (2008) Evaluating frontal and parietal contributions to spatial working memory with repetitive transcranial magnetic stimulation. Brain Res 1230:202–210

Jakobs O, Langner R, Caspers S, Roski C, Cieslik EC, Zilles K, Laird AR, Fox PT, Eickhoff SB (2012) Across-study and within-subject functional connectivity of a right temporo-parietal junction subregion involved in stimulus-context integration. NeuroImage 60:2389–2398

Kim JS, Singh V, Lee JK, Lerch J, Ad-Dab'bagh Y, MacDonald D, Lee JM, Kim SI, Evans AC (2005) Automated 3-D extraction and evaluation of the inner and outer cortical surfaces using a Laplacian map and partial volume effect classification. Neuroimage 27:210–221

Koechlin E, Summerfield C (2007) An information theoretical approach to prefrontal executive function. Trends Cogn Sci 11:229–235

Koechlin E, Basso G, Pietrini P, Panzer S, Grafman J (1999) The role of the anterior prefrontal cortex in human cognition. Nature 399:148–151

Koechlin E, Ody C, Kouneiher F (2003) The architecture of cognitive control in the human prefrontal cortex. Science 302:1181–1185

Laird AR, Eickhoff SB, Li K, Robin DA, Glahn DC, Fox PT (2009) Investigating the functional heterogeneity of the default mode network using coordinate-based meta-analytic modeling. J Neurosci Off J Soc Neurosci 29:14496–14505

Laird AR, Eickhoff SB, Fox PM, Uecker AM, Ray KL, Saenz JJ, McKay DR, Bzdok D, Laird RW, Robinson JL, Turner JA, Turkeltaub PE, Lancaster JL, Fox PT (2011) The BrainMap strategy for standardization, sharing, and meta-analysis of neuroimaging data. BMC Res Notes 4:349

Lancaster JL, Tordesillas-Gutiérrez D, Martinez M, Salinas F, Evans A, Zilles K, Mazziotta JC, Fox PT (2007) Bias between MNI and Talairach coordinates analyzed using the ICBM-152 brain template. Hum Brain Mapp 28:1194–1205

Langner R, Rottschy C, Laird AR, Fox PT, Eickhoff SB (2014) Meta-analytic connectivity modeling revisited: controlling for activation base rates. NeuroImage 99:559–570

Lee S-H, Kravitz DJ, Baker CI (2013) Goal-dependent dissociation of visual and prefrontal cortices during working memory. Nat Neurosci 16:997–999

Lisman J (2005) The theta/gamma discrete phase code occuring during the hippocampal phase precession may be a more general brain coding scheme. Hippocampus 15:913–922

Lückmann HC, Jacobs HIL, Sack AT (2014) The cross-functional role of frontoparietal regions in cognition: internal attention as the overarching mechanism. Prog Neurobiol 116:66–86

Makeig S, Delorme A, Westerfield M, Jung T-P, Townsend J, Courchesne E, Sejnowski TJ (2004) Electroencephalographic brain dynamics following manually responded visual targets. PLoS Biol 2:e176

Mars RB, Neubert F-X, Noonan MP, Sallet J, Toni I, Rushworth MFS (2012) On the relationship between the "default mode network" and the "social brain". Front. Hum, Neurosci **6**

Mason MF, Norton MI, Horn JDV, Wegner DM, Grafton ST, Macrae CN (2007) Wandering minds: the default network and stimulus-independent thought. Science 315:393–395

Mohanty A, Engels AS, Herrington JD, Heller W, Ho M-HR, Banich MT, Webb AG, Warren SL, Miller GA (2007) Differential engagement of anterior cingulate cortex subdivisions for cognitive and emotional function. Psychophysiology 44:343–351

Mukherjee P, Chung SW, Berman JI, Hess CP, Henry RG (2008) Diffusion tensor MR imaging and fiber tractography: technical considerations. Am J Neuroradiol 29:843–852

Murphy K, Birn RM, Handwerker DA, Jones TB, Bandettini PA (2009) The impact of global signal regression on resting state correlations: are anti-correlated networks introduced? NeuroImage 44:893–905

Nichols T, Brett M, Andersson J, Wager T, Poline J-B (2005) Valid conjunction inference with the minimum statistic. NeuroImage 25:653–660

Nooner KB, Mennes M, Li Q, Hinz CM, Kaplan MS, Rachlin AB, Cheung B, Yan C, Calhoun V, Courtney W, King M, Kelly AMC, Martino AD, Petkova E, Biswal B, Hoptman MJ, Javitt DC, Milham MP (2012) The NKI-Rockland sample: a model for accelerating the pace of discovery science in psychiatry. Front Neurosci 6:152

Poldrack RA (2006) Can cognitive processes be inferred from neuroimaging data. Trends Cogn Sci 10:59–63

Poldrack RA, Kittur A, Kalar D, Miller E, Seppa C, Gil Y, Parker DS, Sabb FW, Bilder RM (2011) The cognitive atlas: toward a knowledge foundation for cognitive neuroscience. Front Neuroinformatics 5:17

Postle BR, Ferrarelli F, Hamidi M, Feredoes E, Massimini M, Peterson M, Alexander A, Tononi G (2006) Repetitive transcranial magnetic stimulation dissociates working memory manipulation from retention functions in the prefrontal, but not posterior parietal. Cortex J Cogn Neurosci 18:1712–1722

Raichle ME, MacLeod AM, Snyder AZ, Powers WJ, Gusnard DA, Shulman GL (2001) A default mode of brain function. Proc Natl Acad Sci 98:676–682

Reid AT, Evans AC (2013) Structural networks in Alzheimer's disease. Eur Neuropsychopharmacol J Eur Coll Neuropsychopharmacol 23:63–77

Robinson JL, Laird AR, Glahn DC, Lovallo WR, Fox PT (2010) Metaanalytic connectivity modeling: delineating the functional connectivity of the human amygdala. Hum Brain Mapp 31:173–184

Rogalsky C, Matchin W, Hickok G (2008) Broca's area, sentence comprehension, and working memory: an fMRI Study. Front Hum Neurosci 2:14

Rottschy C, Langner R, Dogan I, Reetz K, Laird AR, Schulz JB, Fox PT, Eickhoff SB (2012) Modelling neural correlates of working memory: a coordinate-based meta-analysis. NeuroImage 60:830–846

Rowe JB, Toni I, Josephs O, Frackowiak RSJ, Passingham RE (2000) The prefrontal cortex: response selection or maintenance within working memory? Science 288:1656–1660

Sarnthein J, Petsche H, Rappelsberger P, Shaw GL, von Stein A (1998) Synchronization between prefrontal and posterior association cortex during human working memory. Proc Natl Acad Sci USA 95:7092–7096

Sauseng P, Klimesch W, Schabus M, Doppelmayr M (2005) Fronto-parietal EEG coherence in theta and upper alpha reflect central executive functions of working memory. Int J Psychophysiol 57:97–103

Sauseng P, Hoppe J, Klimesch W, Gerloff C, Hummel FC (2007) Dissociation of sustained attention from central executive functions: local activity and interregional connectivity in the theta range. Eur J Neurosci 25:587–593

Schenk T, McIntosh RD (2010) Do we have independent visual streams for perception and action? Cogn Neurosci 1:52–62

Scheperjans F, Eickhoff SB, Hömke L, Mohlberg H, Hermann K, Amunts K, Zilles K (2008a) Probabilistic maps, morphometry, and variability of cytoarchitectonic areas in the human superior parietal cortex. Cereb Cortex NY N 1991(18):2141–2157

Scheperjans F, Hermann K, Eickhoff SB, Amunts K, Schleicher A, Zilles K (2008b) Observer-independent cytoarchitectonic mapping of the human superior parietal cortex. Cereb Cortex NY N 1991(18):846–867

Schilbach L, Eickhoff SB, Rotarska-Jagiela A, Fink GR, Vogeley K (2008) Minds at rest? Social cognition as the default mode of cognizing and its putative relationship to the "default system" of the brain. Conscious Cogn 17:457–467

Schilbach L, Bzdok D, Timmermans B, Fox PT, Laird AR, Vogeley K, Eickhoff SB (2012) Introspective minds: using ALE meta-analyses to study commonalities in the neural correlates of emotional processing, social and unconstrained cognition. PLoS One 7:e30920

Smith SM, Nichols TE (2009) Threshold-free cluster enhancement: addressing problems of smoothing, threshold dependence and localisation in cluster inference. NeuroImage 44:83–98

Smith SM, Miller KL, Moeller S, Xu J, Auerbach EJ, Woolrich MW, Beckmann CF, Jenkinson M, Andersson J, Glasser MF, Essen DCV, Feinberg DA, Yacoub ES, Ugurbil K (2012) Temporally-independent functional modes of spontaneous brain activity. Proc Natl Acad Sci 109:3131–3136

Spreng RN, Grady CL (2009) Patterns of Brain Activity Supporting Autobiographical Memory, Prospection, and Theory of Mind, and Their Relationship to the Default Mode Network. J Cogn Neurosci 22:1112–1123

Sridharan D, Levitin DJ, Menon V (2008) A critical role for the right fronto-insular cortex in switching between central-executive and default-mode networks. Proc Natl Acad Sci 105:12569–12574

Stuss DT (2006) Frontal lobes and attention: processes and networks, fractionation and integration. J Int Neuropsychol Soc 12:261–271

Turkeltaub PE, Eden GF, Jones KM, Zeffiro TA (2002) Meta-analysis of the functional neuroanatomy of single-word reading: method and validation. NeuroImage 16:765–780

Turkeltaub PE, Eickhoff SB, Laird AR, Fox M, Wiener M, Fox P (2012) Minimizing within-experiment and within-group effects in Activation Likelihood Estimation meta-analyses. Hum Brain Mapp 33:1–13

Van Essen DC (2004) Surface-based approaches to spatial localization and registration in primate cerebral cortex. NeuroImage 23(Supplement 1):S97–S107

Weissenbacher A, Kasess C, Gerstl F, Lanzenberger R, Moser E, Windischberger C (2009) Correlations and anticorrelations in resting-state functional connectivity MRI: A quantitative comparison of preprocessing strategies. NeuroImage 47:1408–1416

Weissman DH, Roberts KC, Visscher KM, Woldorff MG (2006) The neural bases of momentary lapses in attention. Nat Neurosci 9:971–978

Wright IC, Sham P, Murray RM, Weinberger DR, Bullmore ET (2002) Genetic contributions to regional variability in human brain structure: methods and preliminary results. Neuroimage 17:256–271

Zu Eulenburg P, Caspers S, Roski C, Eickhoff SB (2012) Meta-analytical definition and functional connectivity of the human vestibular cortex. NeuroImage 60:162–169